



HAL
open science

Nonlinear observer design for vehicle lateral load transfer ratio estimation

Shengya Meng, Fanwei Meng, Fan Zhang, Marouane Alma, Madjid Haddad,
Ali Zemouche

► **To cite this version:**

Shengya Meng, Fanwei Meng, Fan Zhang, Marouane Alma, Madjid Haddad, et al.. Nonlinear observer design for vehicle lateral load transfer ratio estimation. American Control Conference, ACC 2024, Jul 2024, Toronto, Canada. 10.23919/ACC60939.2024.10645059 . hal-04727281

HAL Id: hal-04727281

<https://hal.univ-lorraine.fr/hal-04727281v1>

Submitted on 9 Oct 2024

HAL is a multi-disciplinary open access archive for the deposit and dissemination of scientific research documents, whether they are published or not. The documents may come from teaching and research institutions in France or abroad, or from public or private research centers.

L'archive ouverte pluridisciplinaire **HAL**, est destinée au dépôt et à la diffusion de documents scientifiques de niveau recherche, publiés ou non, émanant des établissements d'enseignement et de recherche français ou étrangers, des laboratoires publics ou privés.

Nonlinear Observer Design for Vehicle Lateral Load Transfer Ratio Estimation

S. Meng¹, F. Meng², F. Zhang³, M. Alma¹, M. Haddad⁴ A. Zemouche¹

Abstract—This paper proposes a nonlinear observer design for estimating the lateral load transfer ratio (LTR), a type of rollover index for vehicle safety, with a reduced reliance on measurable signals, applicable to both untripped and tripped rollovers. The dynamics of the four-degree-of-freedom vehicle are modeled to include tripped rollover, treating tire forces as unknown inputs. To address output nonlinearity, the observer employs a generalized inverse, offering an innovative solution. Benefiting from the unique structure of the state-space equations of the vehicle model, only three measurable signals are required for state and unknown input estimation. An algorithm for the observer is presented, ensuring the asymptotic stability of error through parametric solutions for matrix equations and the Lyapunov stability theorem. Validation conducted via CarSim simulations demonstrates the effectiveness of the proposed nonlinear observer in accurately estimating the vehicle states and tire forces. This accuracy positions it as a valuable tool for rollover prediction in vehicle safety applications.

Index Terms—Lateral load transfer ratio, rollover index estimation, nonlinear observer, nonlinear outputs, autonomous vehicle

I. INTRODUCTION

As autonomous driving technology advances, proactive rollover prevention systems have gained prominence for ensuring vehicle safety [1], [2]. Vehicles are susceptible to rollovers, especially during sharp turns, owing to excessive lateral acceleration, commonly referred to as untripped rollovers. Conversely, high-speed vehicles encountering unexpected external factors, such as obstacles or veering off the road, face an increased risk of rollovers, referred to as tripped rollovers [3], [4]. Accurately predicting both types of rollovers serves as a fundamental requirement for effective rollover prevention systems [5].

The lateral load transfer ratio (LTR) is a widely-used rollover index for evaluating the risk of vehicle rollovers [6]. It quantifies the difference in forces between the left and right tires relative to the total force on both sets of tires [7]. This ratio provides a crucial understanding of the lateral load distribution on the vehicle's tires, a key factor in assessing vehicle stability and susceptibility to rollovers [8]. However, real-time estimation of LTR poses a significant challenge due to the unavailability of tire force measurements.

*This work was partially supported by the ANR agency under the project ArtSMo ANR-20-CE48-0015. The authors would also like to acknowledge SEGULA Engineering for its financial support.

¹ Université de Lorraine, 186 rue de Lorraine, CRAN UMR CNRS 7039, Cosnes et Romain 54400, France. (shengyameng.ac@gmail.com)

² School of Control Engineering, Northeastern University at Qinhuangdao, Qinhuangdao, 066000 China.

³ School of Aeronautics and Astronautics, Sun Yat-sen University, Shenzhen 518107, China.

⁴ SEGULA Engineering, 19 rue d'Arras, 92000 Nanterre, France.

In response to the challenge of tire force measurement, researchers have developed various algorithms for real-time LTR estimation [9]. An adaptive Kalman filter, in conjunction with a Butterworth filter, facilitated real-time LTR estimation in [10]. A simplified LTR as a rollover index was employed in [11], taking into consideration the road slope angle. LTR improvement was addressed, and a low-cost unknown input observer (UIO) was introduced to estimate the vehicle's state even in the presence of uncertain disturbances, such as road irregularities, enabling LTR estimation in scenarios involving both tripped and untripped rollovers in [12].

In this study, we design a nonlinear observer to estimate the LTR by introducing a novel representation of state-space equations governing vehicle dynamics, utilizing a four-degree-of-freedom model. The inherent nonlinear outputs are preserved without necessitating additional transformations. To counteract the impact of output nonlinearity, we creatively integrate the generalized inverse operation of matrices within the observer's framework. Furthermore, our innovative observer distinguishes itself from previous research by reducing the required number of measured signals for LTR estimation to only three. The conditions for the observer estimation error converging to zeros are established by linear matrix inequalities (LMIs), relying on parameter solutions from matrix equations and Lyapunov stability theorem. To evaluate our proposed observer's performance, we conducted simulations using CarSim software, demonstrating its high effectiveness in LTR estimation.

In this paper, we adopt the following notation: M^+ denotes the generalized inverse matrix of matrix M , adhering to the condition $MM^+M = M$. I represents the identity matrix with dimensions suitable for the context.

II. THE DYNAMIC MODEL OF VEHICLE

A half-car model is utilized to estimate the rollover index for a vehicle, as depicted in Fig. 1. The model encompasses four degrees of freedom, namely the heave z_s , roll angle ϕ , and the vertical motions of each unsprung mass, z_{ur} and z_{ul} [7].

In this model, the spring mass m_s represents the vehicle body, while the unsprung mass m_u consists of m_{ur} and m_{ul} , representing the mass associated with the axles and tires. The parameter h_R denotes the height of the center of gravity from the roll center. I_z corresponds to the roll moment of inertia, and l_s represents the distance between the left and right suspension locations. The suspension damping coefficient and the suspension stiffness are denoted by d and k , respectively.

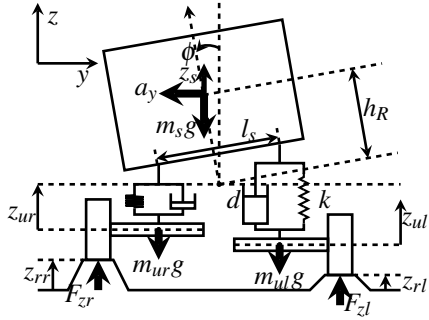


Fig. 1. Four degrees of freedom vehicle model.

Notably, in this model, it takes into account the right and left road displacement inputs, as indicated by z_{rr} and z_{rl} . Moreover, F_{zr} and F_{zl} represent the total right and left tire forces, respectively. Therefore, this model can be used to estimate the tripped rollovers, making it a valuable tool compared to the one-degree-of-freedom model, which may not account for these important factors [5].

Based on the distinction between the loads on the left and right sides of the vehicle tires, the LTR is defined as follows, as mentioned in [7]:

$$\text{LTR} = \frac{F_{zl} - F_{zr}}{F_{zl} + F_{zr}}, \quad \|\text{LTR}\| \leq 1. \quad (1)$$

When LTR equals 0, it indicates that the vehicle is traveling straight, with equal tire forces on both the left and right sides. On the other hand, if one side of the vehicle experiences a significant reduction in tire force, for instance, due to the lifting of a tire off the ground during a sharp turn or abrupt maneuver, the LTR will approach 1 or -1 .

The definition of LTR as rollover index is indeed concise but can be challenging to implement in practice because measuring the tire forces. Especially when considering the effects of road displacement input, LTR estimation is complex and often requires the use of advanced sensor systems..

To address this challenge, the design of an observer to estimate the total right and left tire forces, F_{zr} and F_{zl} , becomes crucial. Such an observer would enable the estimation of these critical parameters indirectly, based on available sensor measurements and the known dynamics of the vehicle. This estimation process can significantly enhance the practical applicability of LTR as a stability indicator, particularly in real-time vehicle monitoring and control systems.

The right and left tire forces of the vehicle, represented as F_{zr} and F_{zl} , are treated as unknown inputs denoted by the vector $\mu = [F_{zr} \ F_{zl}]^T$. The state variable is defined as $x = [z_s - z_{ur} \ \dot{z}_s - \dot{z}_{ur} \ z_s - z_{ul} \ \dot{z}_s - \dot{z}_{ul} \ \phi \ \dot{\phi}]^T$. Then, the dynamic model of vehicle can be written as [13]:

$$\dot{x} = \bar{A}x + \alpha(x) + \bar{B}\mu, \quad (2a)$$

$$z = Ex + \beta(x) + b\mu, \quad (2b)$$

$$y = Cx + \Psi(x), \quad (2c)$$

where

$$\bar{A} = \begin{bmatrix} 0 & 1 & 0 & 0 & 0 & 0 \\ -\frac{k}{m_s} - \frac{k}{m_u} & -\frac{d}{m_s} - \frac{d}{m_u} & -\frac{k}{m_s} & -\frac{d}{m_s} & 0 & 0 \\ 0 & 0 & 0 & 1 & 0 & 0 \\ -\frac{k}{m_s} & -\frac{d}{m_s} & -\frac{k}{m_s} - \frac{k}{m_u} & -\frac{d}{m_s} - \frac{d}{m_u} & 0 & 0 \\ 0 & 0 & 0 & 0 & 0 & 1 \\ \frac{kl_s}{2I_z} & \frac{dl_s}{2I_z} & -\frac{kl_s}{2I_z} & -\frac{dl_s}{2I_z} & 0 & 0 \end{bmatrix}$$

$$\alpha(x) = \begin{bmatrix} 0 \\ \frac{kl_s}{2m_u} \sin \phi + \frac{dl_s}{2m_u} \dot{\phi} \cos \phi \\ 0 \\ -\frac{kl_s}{2m_u} \sin \phi - \frac{dl_s}{2m_u} \dot{\phi} \cos \phi \\ 0 \\ \frac{m_s a_y h_R}{I_z} \cos \phi + \left(\frac{m_s g h_R}{I_z} - \frac{kl_s^2}{2I_z} \right) \sin \phi - \frac{dl_s^2}{2I_z} \dot{\phi} \cos \phi \end{bmatrix}$$

$$\bar{B} = \begin{bmatrix} 0 & \frac{1}{m_u} & 0 & 0 & 0 & 0 \\ 0 & 0 & 0 & \frac{1}{m_u} & 0 & 0 \end{bmatrix}^T$$

$$E = \begin{bmatrix} \frac{k}{m_u} & \frac{d}{m_u} & 0 & 0 & 0 & 0 \\ 0 & 0 & \frac{k}{m_u} & \frac{d}{m_u} & 0 & 0 \end{bmatrix}, \quad C = \begin{bmatrix} 1 & 0 & 0 & 0 & 0 & 0 \\ 0 & 0 & 0 & 0 & 0 & 1 \end{bmatrix}$$

$$\beta(x) = \begin{bmatrix} -\frac{kl_s}{2m_u} \sin \phi - \frac{dl_s}{2m_u} \dot{\phi} \cos \phi \\ \frac{kl_s}{2m_u} \sin \phi + \frac{dl_s}{2m_u} \dot{\phi} \cos \phi \end{bmatrix} \quad b = \begin{bmatrix} -\frac{1}{m_u} & 0 \\ 0 & -\frac{1}{m_u} \end{bmatrix}$$

$$C = \begin{bmatrix} 1 & 0 & 0 & 0 & 0 & 0 \\ 0 & 0 & 0 & 0 & 0 & 1 \end{bmatrix} \quad \Psi(x) = \begin{bmatrix} -\frac{l_s}{2} \sin \phi \\ 0 \end{bmatrix}$$

and the measurable outputs z and y are

$$z = \begin{bmatrix} \ddot{z}_{ur} \\ \ddot{z}_{ul} \end{bmatrix}, \quad y = \begin{bmatrix} z_s - z_{ur} - \frac{l_s}{2} \sin \phi \\ \dot{\phi} \end{bmatrix}.$$

Since the matrix b is invertible, the unknown input variable μ can be expressed as follows:

$$\mu = b^{-1}(z - Ex - \beta(x)), \quad (3)$$

From the above equation, if the state vector x is known, the unknown input variable μ can be computed.

By substituting (3) into (2a), we obtain

$$\begin{aligned} \dot{x} &= \bar{A}x + \alpha(x) + \bar{B}b^{-1}(z - Ex - \beta(x)) \\ &= (\bar{A} - \bar{B}b^{-1}E)x + \bar{B}b^{-1}z + \alpha(x) - \bar{B}b^{-1}\beta(x). \end{aligned} \quad (4)$$

In accordance with (4), (2a) and (2c) can be rewritten as follows:

$$\begin{aligned} \dot{x} &= Ax + Bz + D_f f(F_l x), \\ y &= Cx + D_g g(x), \end{aligned} \quad (5)$$

where

$$A = \bar{A} - \bar{B}b^{-1}E, \quad B = \bar{B}b^{-1}, \quad D_f = [0 \ 0 \ 0 \ 0 \ 0 \ 1]^T,$$

$$D_g = [1 \ 0]^T, \quad g(x) = -\frac{l_s}{2} \sin \phi,$$

$$f(F_l x) = \frac{m_s a_y h_R}{I_z} \cos \phi + \left(\frac{m_s g h_R}{I_z} - \frac{kl_s^2}{2I_z} \right) \sin \phi - \frac{dl_s^2}{2I_z} \dot{\phi} \cos \phi. \quad (6)$$

Prior to designing the observer, it is imperative that the following assumptions be met:

Assumption 1: The function $f(F_l x)$ satisfies the following Lipschitz condition:

$$\|f(F_l x_1) - f(F_l x_2)\| \leq \lambda \|F_l(x_1 - x_2)\|, \quad (7)$$

where λ represents the Lipschitz constant.

Assumption 2: There exists a matrix W such that:

$$\text{rank} \begin{bmatrix} W \\ \bar{C} \end{bmatrix} = n, \quad \bar{C} = (I - D_g D_g^+) C. \quad (8)$$

These two assumptions are not definitely strict. It is evident that Assumptions 1 and 2 are satisfied based on (6).

III. NONLINEAR OBSERVER DESIGN

Our objective is the design of a nonlinear observer for system (5) given by the following form:

$$\begin{aligned} \dot{\zeta} &= N\zeta + Jz + F(I - D_g D_g^+)y + TD_f f(F_l \hat{x}) \\ \hat{x} &= P\zeta + Q(I - D_g D_g^+)y \end{aligned} \quad (9)$$

where $\zeta \in \mathbb{R}^q$ is the state vector of the observer, $\hat{x} \in \mathbb{R}^n$ is the estimated state vector of x , and N, J, F, T, P and Q are undetermined matrices with dimensions suitable for the problem at hand.

Remark 1: The particular structure of the observer, incorporating the generalized inverse operation of matrices D_g , enables the accommodation of fewer measurable outputs than [13]. This is attributable to the specific form of the matrix D_g , resulting in $I - D_g D_g^+ = \begin{bmatrix} 0 & 0 \\ 0 & 1 \end{bmatrix}$. Consequently, the measurement signal $y(1) = z_s - z_{ur} - l_s/\sin\phi$ is not necessitated for input into the observer.

Let us define the following two errors $\delta = \zeta - Tx$, and $e = \hat{x} - x$. Subsequently, we derive the error system as follows:

$$\begin{aligned} \dot{\delta} &= \dot{\zeta} - T\dot{x} \\ &= N\zeta + Jz + F(I - D_g D_g^+)y + TD_f f(F_l \hat{x}) \\ &\quad - T(Ax + Bz + D_f f(F_l x)) \\ &= N\zeta - NTx + (J - TB)z + F(I - D_g D_g^+)(Cx + D_g g(x)) \\ &\quad + TD_f \Delta f - TAx + NTx, \\ &= N\delta + (NT + F\bar{C} - TA)x + (J - TB)z + TD_f \Delta f \\ e &= P\zeta + Q(I - D_g D_g^+)y - x - PTx + PTx \\ &= P\delta + (PT + Q\bar{C} - I)x, \end{aligned} \quad (10)$$

where for convenience, we define $\Delta f = f(F_l \hat{x}) - f(F_l x)$.

Remark 2: Based on the previous analysis, it can be inferred that the application of the generalized inverse operation to D_g within the observer (9) effectively mitigates the influence of output nonlinearity on error dynamics. Despite the assertion made in Remark 1 that output nonlinearity is dispensable for the estimation of vehicle states, the distinctive architecture of this observer nonetheless introduces a novel approach for addressing and managing output nonlinearity.

If the following equation holds:

$$NT + F\bar{C} - TA = 0, \quad (11a)$$

$$J = TB, \quad (11b)$$

$$PT + Q\bar{C} = I. \quad (11c)$$

Then, the error system described by (10) can be simplified as follows:

$$\begin{aligned} \dot{\delta} &= N\delta + TD_f \Delta f, \\ e &= P\delta. \end{aligned} \quad (12)$$

Rewrite (11a) and (11c) as

$$\begin{bmatrix} N & F \\ P & Q \end{bmatrix} \begin{bmatrix} T \\ \bar{C} \end{bmatrix} = \begin{bmatrix} TA \\ I \end{bmatrix}. \quad (13)$$

The necessary and sufficient condition for its solution is

$$\text{rank} \begin{bmatrix} T \\ \bar{C} \\ TA \\ I \end{bmatrix} = \text{rank} \begin{bmatrix} T \\ \bar{C} \end{bmatrix} = n. \quad (14)$$

For convenience, define the following two matrices as

$$\mathscr{W} = \begin{bmatrix} W \\ \bar{C} \end{bmatrix}, \quad \mathscr{E} = \begin{bmatrix} I_n \\ \bar{C} \end{bmatrix}. \quad (15)$$

Then, there are matrices T and K that satisfy

$$\begin{bmatrix} T & K \end{bmatrix} \begin{bmatrix} I \\ \bar{C} \end{bmatrix} = W, \quad (16)$$

and the parameterized results of the matrices T and K are

$$T = T_1 - \eta_1 T_2, \quad K = K_1 - \eta_1 K_2, \quad (17)$$

where the matrices T_1, T_2, K_1 and K_2 are as follows:

$$\begin{aligned} T_1 &= W\mathscr{E}^+ \begin{bmatrix} I \\ 0 \end{bmatrix}, \quad T_2 = (I - \mathscr{E}\mathscr{E}^+) \begin{bmatrix} I \\ 0 \end{bmatrix}, \\ K_1 &= W\mathscr{E}^+ \begin{bmatrix} 0 \\ I \end{bmatrix}, \quad K_2 = (I - \mathscr{E}\mathscr{E}^+) \begin{bmatrix} 0 \\ I \end{bmatrix}. \end{aligned} \quad (18)$$

From (16) and (11a), there is $NW - F\bar{C} - NK\bar{C} = TA$, which can be rewritten as

$$\begin{bmatrix} N & F \\ 0 & I \end{bmatrix} \begin{bmatrix} I & -K \\ 0 & I \end{bmatrix} \mathscr{W} = TA.$$

The matrices N and F can be expressed as

$$\begin{aligned} N &= N_1 - \eta_1 N_2 - \eta_2 N_3, \\ F &= F_1 - \eta_1 F_2 - \eta_2 F_3, \end{aligned} \quad (19)$$

where η_2 is a parameter matrix, and the matrices N_1, N_2, N_3, F_1, F_2 and F_3 are

$$\begin{aligned} N_1 &= T_1 A \mathscr{W}^+ \begin{bmatrix} I \\ 0 \end{bmatrix}, \quad N_2 = T_2 A \mathscr{W}^+ \begin{bmatrix} I \\ 0 \end{bmatrix}, \\ N_3 &= (I - \mathscr{W}\mathscr{W}^+) \begin{bmatrix} I \\ 0 \end{bmatrix}, \quad F_1 = T_1 A \mathscr{W}^+ \begin{bmatrix} K \\ I \end{bmatrix}, \\ F_2 &= T_2 A \mathscr{W}^+ \begin{bmatrix} K \\ I \end{bmatrix}, \quad F_3 = (I - \mathscr{W}\mathscr{W}^+) \begin{bmatrix} K \\ I \end{bmatrix}. \end{aligned} \quad (20)$$

Similarly, the matrices P and Q are

$$P = P_1 - \eta_3 P_3, \quad Q = Q_1 - \eta_3 Q_3, \quad (21)$$

where η_3 is a parameter matrix, and P_1 and Q_1 are as follows:

$$P_1 = \mathscr{W}^+ \begin{bmatrix} I \\ 0 \end{bmatrix}, \quad Q_1 = \mathscr{W}^+ \begin{bmatrix} K \\ I \end{bmatrix}. \quad (22)$$

Using this parameterization, we can address the following theorem.

Theorem 1: For a nonlinear system (5), if there exist positive definite matrices X and a positive constant $\rho < 1$,

along with matrices of appropriate dimensions Y_1, Y_2 and η_3 satisfying the following LMIs

$$\begin{bmatrix} M_{11} & M_{12} & M_{13} \\ M_{12}^T & -\rho & 0 \\ M_{13}^T & 0 & -(I + \lambda^2 F_l^T F_l)^{-1} \end{bmatrix} < 0, \quad (23)$$

where

$$\begin{aligned} M_{11} &= XN_1 + N_1^T X - Y_1 N_2 - N_2^T Y_1^T - Y_2 N_3 - N_3^T Y_2^T, \\ M_{12} &= XT_1 D_f - Y_1 T_2 D_f, \quad M_{13} = P_1^T - N_3^T \eta_3^T, \end{aligned}$$

then there is a nonlinear observer in the form of (9) with (13) such that the error system (12) asymptotically converges to zero.

Proof 1: Let $Y_1 = X\eta_1$ and $Y_2 = X\eta_2$. From the LMIs (23) and the parameters solutions of N, T, P as shown in (17), (19), and (21), there are the following matrix inequalities

$$\begin{bmatrix} N^T X + XN & X(TD_f) & P^T \\ (TD_f)^T X & -\rho & 0 \\ P & 0 & -(I + \lambda^2 F_l^T F_l)^{-1} \end{bmatrix} < 0, \quad (24)$$

Choose the Lyapunov function as $V = \delta^T X \delta$, there is

$$\begin{aligned} \dot{V} &= \delta^T X \dot{\delta} + \delta^T X \dot{\delta} \\ &= \delta^T (N^T X + XN) \delta + \Delta f^T (TD_f)^T X \delta + \delta^T X (TD_f) \Delta f \\ &= \delta^T (N^T X + XN) \delta + \Delta f^T (TD_f)^T X \delta + \delta^T X (TD_f) \Delta f \\ &\quad + \Delta f^T \rho \Delta f - \Delta f^T \rho \Delta f \\ &< \delta^T (N^T X + XN) \delta + \Delta f^T (TD_f)^T X \delta + \delta^T X (TD_f) \Delta f \\ &\quad + \Delta f^T \Delta f - \Delta f^T \rho \Delta f \end{aligned}$$

Here $\rho < 1$ is applied. Due to the Lipschitz nonlinear function $f(F_l x)$, we have $\Delta f^T \Delta f < \lambda^2 e^T F_l^T F_l e$. Further,

$$\begin{aligned} \dot{V} &< \delta^T (N^T X + XN) \delta + \Delta f^T (TD_f)^T X \delta + \delta^T X (TD_f) \Delta f \\ &\quad + \lambda^2 e^T F_l^T F_l e - \Delta f^T \rho \Delta f \\ &< \delta^T (N^T X + XN + P^T ((I + \lambda^2 F_l^T F_l)) P) \delta + \Delta f^T (TD_f)^T X \delta \\ &\quad + \delta^T X (TD_f) \Delta f - \Delta f^T \rho \Delta f \\ &= \begin{bmatrix} \delta \\ \Delta f \end{bmatrix}^T \begin{bmatrix} N^T X + XN + P^T (I + \lambda^2 F_l^T F_l) P & X(TD_f) \\ (TD_f)^T X & -\rho \end{bmatrix} \begin{bmatrix} \delta \\ \Delta f \end{bmatrix} P = \end{aligned}$$

According to the Schur Complement Lemma and matrix inequalities (24), there is $\dot{V} < 0$. Therefore, the error system (12) is asymptotically stable. The proof is completed. ■

IV. SIMULATION

This section presents the simulation results obtained by applying the algorithm described in Theorem 1. The vehicle model used in these simulations is a standard SUV sourced from CarSim. The parameters of the vehicle model are $m_s = 1592$ kg, $m_u = 80$ kg, $h_R = 0.73$ m, $I_z = 614$ kg · m², $g = 9.81$ m/s, $k = 260000$ N/m, $l_s = 1.565$ m, $d = 4800$ kg/s.

During the simulation, we consider a scenario in which the SUV vehicle encounters road bumps while cornering. The resulting lateral acceleration and the road displacement inputs in this scenario is depicted in Fig. 2.

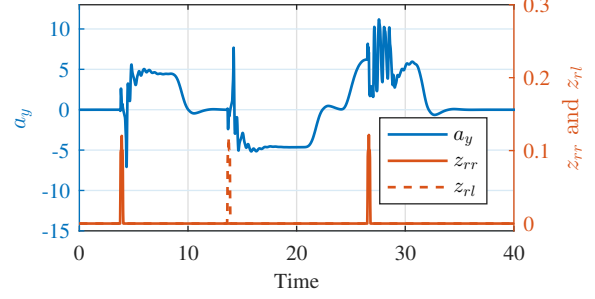


Fig. 2. Lateral acceleration input and the road displacement input.

For convenience, we select the matrix W to be an identity matrix. Applying Theorem 1 to the vehicle model (5), the designed matrices in the observer (9) are determined to be:

$$\begin{aligned} N &= \begin{bmatrix} -0.446 & 0.992 & 0.446 & 0.008 & 0 & -0.027 \\ -163.935 & -3.026 & -162.698 & -3.004 & 0 & 2.513 \\ 0.447 & 0.008 & -0.447 & 0.992 & 0 & -0.023 \\ -162.654 & -3.003 & -163.980 & -3.027 & 0 & 2.609 \\ 0 & 0 & 0 & 0 & 0 & 0 \\ -0.014 & 0 & 0.014 & 0 & 0 & -1.511 \end{bmatrix}, \\ J &= \begin{bmatrix} 0 & 0 \\ 1 & 0 \\ 0 & 0 \\ 0 & 1 \\ 0 & 0 \\ 0 & 0 \\ 0 & 0 \end{bmatrix}, \quad T = \begin{bmatrix} 1 & 0 & 0 & 0 & 0 & -0.001 \\ 0 & 1 & 0 & 0 & 0 & -0.002 \\ 0 & 0 & 1 & 0 & 0 & 0.001 \\ 0 & 0 & 0 & 1 & 0 & 0.002 \\ 0 & 0 & 0 & 0 & 1 & 0 \\ 0 & 0 & 0 & 0 & 0 & 0 \end{bmatrix}, \\ F &= \begin{bmatrix} -0.013 & 0.001 \\ 0.076 & -0.001 \\ -0.013 & -0.001 \\ 0.076 & 0.002 \\ 0 & 1 \\ 0 & 0 \end{bmatrix}, \quad Q = \begin{bmatrix} 1 & 0.001 \\ -1.013 & 0.002 \\ 1 & -0.001 \\ -1.013 & -0.002 \\ 1 & 0 \\ 1 & 1 \end{bmatrix}, \\ &= \begin{bmatrix} 1 & 0 & 0 & 0 & 0 & 0.015 \\ 0 & 1 & 0 & 0 & 0 & -0.469 \\ 0 & 0 & 1 & 0 & 0 & 0.017 \\ 0 & 0 & 0 & 1 & 0 & -0.619 \\ 0 & 0 & 0 & 0 & 1 & -0.029 \\ 0 & 0 & 0 & 0 & 0 & 0.001 \end{bmatrix}. \end{aligned} \quad (25)$$

The estimated results are displayed in Fig. 3. While these figures reveal that there are still some discrepancies between the actual values and the estimated values, it's important to note that the observer is built upon a four-degree-of-freedom vehicle model, whereas the actual vehicle model has a greater number of degrees of freedom. Despite this disparity, the estimated states closely approximate the actual values, underscoring the effectiveness of the observer.

The unknown input μ and its estimates are depicted in Fig. 4. Additionally, the LTR and its estimates are presented in Fig. 5. It's noteworthy that the estimation error is minimal, demonstrating that the provided estimates are sufficient for preventing rollover in the vehicle.

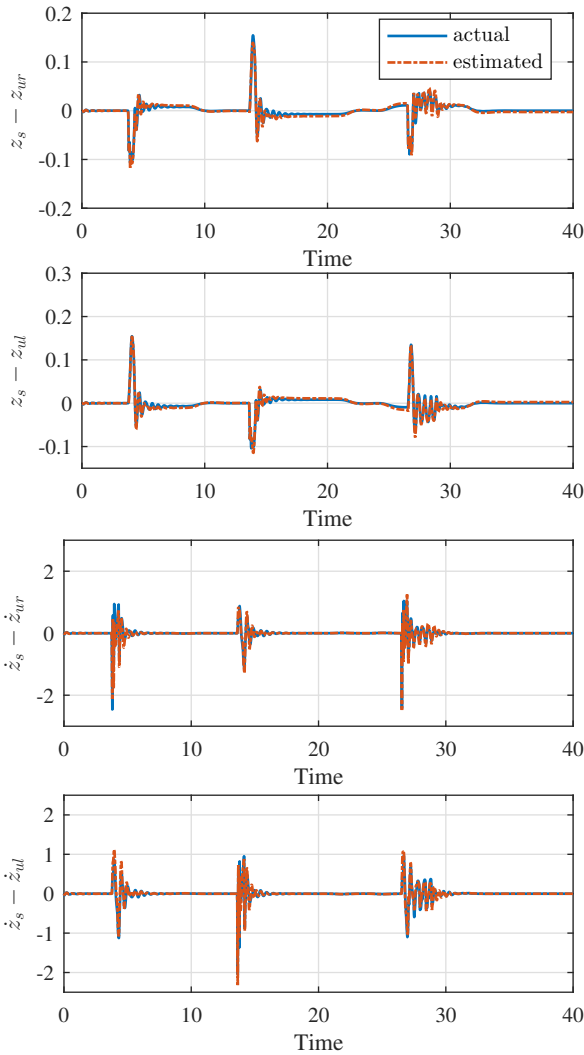


Fig. 3. States estimated results.

V. CONCLUSIONS

This paper develops a novel nonlinear observer for LTR estimation, requiring fewer measurable signals and applicable to both untripped and tripped rollovers. Our approach retains inherent output nonlinearities without additional transformations, effectively addressing this challenge. The conditions for observer error convergence is established by the parametric solutions for matrix equations and the Lyapunov stability theorem. In future, we aim to develop our strategy with intelligent algorithms, such as neural networks, to enhance robustness against inaccuracies in the model.

REFERENCES

- [1] M. Ataei, A. Khajepour, and S. Jeon, "Model predictive rollover prevention for steer-by-wire vehicles with a new rollover index," *International Journal of Control*, vol. 93, no. 1, pp. 140–155, 2020.
- [2] G. Phanomchoeng, A. Zemouche, and R. Rajamani, "Real-time automotive slip angle estimation with extended h_∞ circle criterion observer for nonlinear output system," in *2017 American Control Conference (ACC)*. IEEE, 2017, pp. 1636–1641.
- [3] G. Phanomchoeng and R. Rajamani, "New rollover index for the detection of tripped and untripped rollovers," *IEEE Transactions on Industrial Electronics*, vol. 60, no. 10, pp. 4726–4736, 2012.

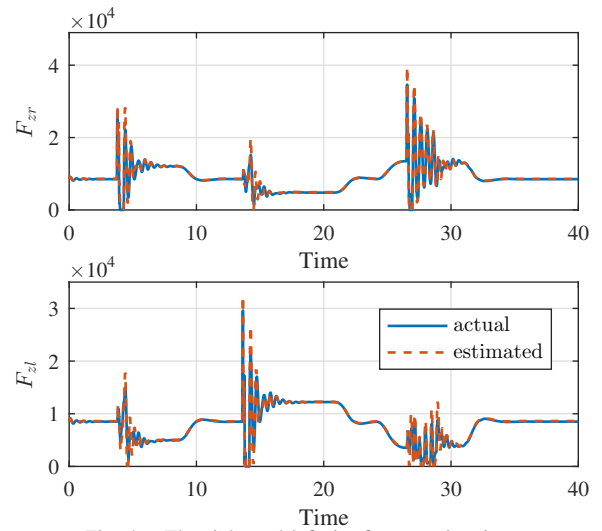


Fig. 4. The right and left tire forces estimation.

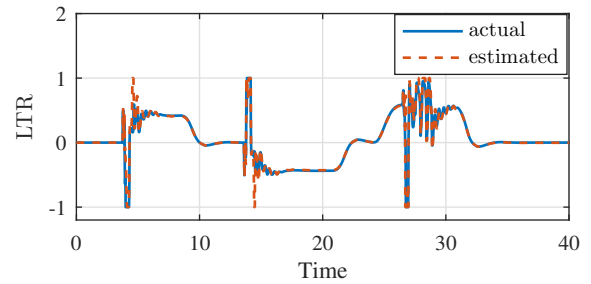


Fig. 5. The rollover index and its estimation.

- [4] F. Wang and Y. Chen, "Vehicle rollover propensity detection based on a mass-center-position metric: A continuous and completed method," *IEEE Transactions on Vehicular Technology*, vol. 68, no. 9, pp. 8652–8662, 2019.
- [5] G. Phanomchoeng, K. Treetipsounthorn, S. Chantranuwathana, and L. Wuttisittikulij, "Untripped and tripped rollovers with a neural network," *International Journal of Automotive Technology*, vol. 24, no. 3, pp. 811–828, 2023.
- [6] H. Imine and M. Djemai, "Switched control for reducing impact of vertical forces on road and heavy-vehicle rollover avoidance," *IEEE Transactions on Vehicular Technology*, vol. 65, no. 6, pp. 4044–4052, 2015.
- [7] R. Rajamani, *Vehicle dynamics and control*. Springer Science & Business Media, 2011.
- [8] X. Ding, L. Zhang, Z. Wang, and P. Liu, "Acceleration slip regulation for four-wheel-independently-actuated electric vehicles based on road identification through the fuzzy logic," *IFAC-PapersOnLine*, vol. 51, no. 31, pp. 943–948, 2018.
- [9] D. Chu, Z. Li, J. Wang, C. Wu, and Z. Hu, "Rollover speed prediction on curves for heavy vehicles using mobile smartphone," *Measurement*, vol. 130, pp. 404–411, 2018.
- [10] C. Wang, Z. Wang, L. Zhang, D. Cao, and D. G. Dorrell, "A vehicle rollover evaluation system based on enabling state and parameter estimation," *IEEE Transactions on Industrial Informatics*, vol. 17, no. 6, pp. 4003–4013, 2020.
- [11] D. Shin, S. Woo, and M. Park, "Rollover index for rollover mitigation function of intelligent commercial vehicle's electronic stability control," *Electronics*, vol. 10, no. 21, p. 2605, 2021.
- [12] X. Yang, C. Wu, Y. He, X.-Y. Lu, and T. Chen, "A dynamic rollover prediction index of heavy-duty vehicles with a real-time parameter estimation algorithm using nlms method," *IEEE Transactions on Vehicular Technology*, vol. 71, no. 3, pp. 2734–2748, 2022.
- [13] G. Phanomchoeng and R. Rajamani, "Real-time estimation of rollover index for tripped rollovers with a novel unknown input nonlinear observer," *IEEE/ASME Transactions on Mechatronics*, vol. 19, no. 2, pp. 743–754, 2013.